**IET Systems Biology**

## ORIGINAL RESEARCH

# Comprehensive analysis of alternative splicing signatures in pancreatic head cancer

Lingshan Zhou[1] | Yuan Yang[2,3,4] | Jian Ma[5] | Min Liu[3,4] | Rong Liu[1] |
Xiaopeng Ma[2,5] | Chengdong Qiao[1]

[1]Department of Geriatrics Ward 2, the First Hospital of Lanzhou University, Lanzhou, China

[2]The First Clinical Medical College, Lanzhou University, Lanzhou, China

[3]Department of Gastroenterology, the First Hospital of Lanzhou University, Lanzhou, China

[4]Gansu Key Laboratory of Gastroenterology, Lanzhou University, Lanzhou, China

[5]Department of General Surgery, the First Hospital of Lanzhou University, Lanzhou, China

**Correspondence**

Chengdong Qiao, Department of Geriatrics Ward 2, the First Hospital of Lanzhou University, Lanzhou 730030, China.
Email: qcd2000@163.com

## Abstract

The correlation between dysregulation of splicing and cancers has been increasingly recognised and confirmed. The identification of valuable alternative splicing (AS) in pancreatic head cancer (PHC) has a great significance. AS profiles in PHC were generated using the data from The Cancer Genome Atlas and TCGASpliceSeq. Then, the NMF clustering method was performed to identify overall survival-associated AS (OS-AS) subtypes in PHC patients. Subsequently, we used least absolute shrinkage and selection operator Cox regression analysis to construct an AS-related risk model. The splicing regulatory network was uncovered by Cytoscape 3.7. A total of 1694 OS-AS events were obtained. The PHC patients were divided into clusters 1 and 2. Cluster 1 had poorer prognosis and lower infiltration of immune cells. Subsequently, a prognostic signature was established that showed good performance in predicting OS and progression-free survival. The risk score of this signature was associated with the unique tumour immunity. Moreover, a nomogram incorporating the risk score and clinicopathological parameters was established. Finally, a splicing factor-AS regulatory network was developed. A comprehensive analysis of the AS events in PHC associated with prognosis and tumour immunity may help provide reliable information to guide individual treatment strategies.

**KEYWORDS**

alternative splicing, immune checkpoints, pancreatic head cancer, prognosis, tumour immune

## 1 | INTRODUCTION

Pancreatic cancer (PC) is a highly heterogeneous malignancy, with a 5-year survival as low as 9% [1]. Despite its relatively low incidence, PC is predicted to become the third leading cause of cancer-related death by 2025 [2]. Over the past decade, no major progress has been made in improving patient outcomes, and a complete resection remains the only potential treatment modality. Unfortunately, a majority of patients with PC present with unresectable disease at initial diagnosis [3]. To date, there are no highly sensitive and accurate biomarkers that can predict the survival of PC, especially pancreatic head cancer (PHC). Hence, it is imperative to search for effective prognostic indicators that

guide clinical decision-making and improve the clinical management of PHC.

PC is divided into head, body, and tail cancers in accordance with anatomy. Ling et al. reported the discovery that different subtypes have showed functional and molecular diversity with respect to tissue composition, vascularisation, and innervations [4]. There has been a long-lasting debate over whether tumour location could influence the development of cancers. Increasing evidence has shown that different tumour localisations in the pancreas display different clinical presentations, treatment efficiencies, and clinical outcomes [5–7]. Several in vitro experiments also confirmed that there are significant differences in chemo- and/or radio resistant, cell migration and invasion, pro-angiogenic potential, and genetic

profiles between pancreatic head and body/tail cancers [4]. With the wide application of a high-throughput sequencing technology, many studies have demonstrated that PC shows interpatient genomic heterogeneity [8, 9]. Dreyer et al. investigated the molecular differences between pancreatic head and body/tail cancers and further elucidated the major signalling pathways of these cancers. In addition, these cancers also show the different features of antitumour immune responses [10]. These findings suggested that the mechanisms in carcinogenesis and tumour progression of PC might differ with tumour localisation and confirmed the great significance of the subsite division. Recent studies have identified various prognostic signatures for PC. However, little is known about the prognostic signature in PHC.

Alternative splicing (AS) is a pervasive gene regulatory process that determines the generation of various transcripts, which contributes to proteome complexity [11]. A growing number of studies have revealed that AS plays an important role in numerous critical biological processes governing many cell fate decisions [12]. In particular, the advances in sequencing technology in the last few years have revealed the potential roles of AS in the aetiology of cancers, including PC [13]. In this regard, aberrations in splicing contribute to pro/antitumour phenotypes in PC by regulating the expression of key genes [14–16]. Additionally, several studies have shown that AS is significantly correlated with the tumour stage and survival in PC [17]. Identifying and characterising dysregulation of AS events in PC might be of significant clinical value regarding the diagnosis and treatment of the disease. Nevertheless, there is no clear explanation for the dysregulation of AS events in PHC.

In the present study, we characterised the different RNA splicing patterns in PHC by using the data from The Cancer Genome Atlas (TCGA) and TCGA SpliceSeq. Two subtypes with distinct tumour immune characteristics were identified based on OS-AS events. We utilised the least absolute shrinkage and selection operator (LASSO) regression model to identify seven OS-AS events in PHC. With this signature, the risk score was calculated and then a prognostic nomogram was developed, which was demonstrated to be a precise predictor for prognosis. Finally, we established a regulatory network of splicing factor (SF) genes and their target AS events to explore the underlying mechanisms in PHC.

## 2 | MATERIALS AND METHODS

### 2.1 | Data source

The RNA-seq transcriptome data and corresponding clinical information regarding PC were downloaded from the TCGA data portal (https://tcga-data.nci.nih.gov/tcga/). A total of 130 PHC samples were extracted using a Perl script. We used the SpliceSeq tool to profile AS patterns in PHC samples (https://bioinformatics.mdanderson.org/TCGASpliceSeq/). The percent spliced in (PSI) value was used to quantify AS events from zero to one [18]. A total of seven types of AS

events were calculated in the present study, including exon skip (ES), mutually exclusive exons (MEs), retained introns (RIs), alternate promoters (APs), alternate terminators (ATs), alternate donor sites (ADs), and alternate acceptor sites (AAs). The intersections of the 7 AS event subtypes were visualised using the 'UpSet' R package.

### 2.2 | Identification of survival-related AS events

We further explored the association between AS events and overall survival (OS) of PHC. The univariate Cox regression analysis was performed to identify OS-associated AS (OS-AS) events with a $p$ value of $< 0.05$. The result was shown by drawing a volcano plot based on the correspondence between the $p$ value and Z-score. Bubble plots are presented to display the top 20 OS-AS events of each splicing pattern. The correlation between AS events and OS of PHC was indicated by the colour gradient and size of bubbles.

### 2.3 | Clustering analysis for OS-AS events

Based on the non-negative matrix factorisation (NMF) clustering of PSI values of OS-AS events, PHC patients were categorised into distinct subtypes for $k = 2$–$10$ by using the 'NMF' R package. The parameter settings were as follows: number of repetitions = 1000, method = 'brunet'. According to the cophenetic correlation coefficient, rss and silhouette, the optimal $k$ value was further determined.

### 2.4 | Exploration of immune infiltration between AS clusters

To assess the immune infiltration between different AS clusters, we performed the microenvironment cell-population (MCP)-counter algorithm to quantify the score of 10 immune cells by using the 'MCPcounter' R package. A previously described immune classification has defined six immune subtypes (C1–C6) in cancer [19]. We further investigated the relationship between the clusters and six immune subtypes. Sankey plots were drawn by using the 'ggalluvial' R package.

### 2.5 | Discovering an AS-based risk score

We used LASSO regression analysis to identify AS events that are correlated with OS from OS-AS events by the 'glmnet' R package. According to the optimal penalty parameter ($\lambda$) value determined by a 10-fold cross-validation (the value of $\lambda$ corresponding to the minimum mean cross-validated error), the prognostic signature was constructed using these filtered AS events. The following formula was used to calculate the risk score of each patient: Risk score $= \sum_{i=1}^{n}(\text{PSI} * \text{LASSO regression coefficient})$. According to the cut-off value determined by using

the 'survminer' R package, PHC patients were divided into high- and low-risk groups. The time-dependent ROC curve is an appropriate tool to evaluate the performance of candidate markers when considering time-to-event data. We used the 'timeROC' R package to assess the predictive potential of the model by measuring the area under the receiver operating characteristic curve (AUC-ROC). Then, the 1-, 2-, and 3-year ROC curves were plotted.

## 2.6 | Survival analysis

A Kaplan–Meier survival curve was applied to evaluate the differences in OS and progression-free survival (PFS) between groups. A log-rank $p < 0.05$ was considered statistically significant.

## 2.7 | Construction of the predictive nomogram

To identify independent prognostic parameters, univariate and multivariate Cox regression analyses were applied accordingly. A $p$ value $< 0.05$ was considered statistically significant. Then, the risk score and clinical parameters were used to develop a prognostic nomogram that might predict the 1-, 2-, and 3-year OS of patients with PHC. A nomogram plot was established by using the 'rms' R package. Calibration curves were generated to assess the predictive validity of the nomogram. A higher degree of consistency with 45° dotted line indicates the optimal predictive performance.

## 2.8 | Analyses of the immune landscape

To explore the differences in the tumour microenvironment between the high- and low-risk groups, we used the 'estimate' R package to compute the ESTIMATE score, stromal score, immune score, and tumour purity for each patient with PHC. Additionally, a single-sample gene set enrichment analysis (ssGSEA) was performed to uncover the characteristics of immune cell infiltration, immune-related pathways and immune-related functions by the 'gsva' R package. A total of 20 major immune checkpoint genes were acquired from a previous study [20]. The correlation between the risk score and the main immune checkpoint genes was calculated by Pearson correlation analysis. The Wilcoxon rank-sum test was used to compare the differences in the expression of 20 immune checkpoint genes between the low- and high-risk groups.

## 2.9 | Construction of the splicing correlation network

A list of 404 SF genes was retrieved from the previous literature [21]. The expression of SF genes was obtained from level 3 mRNA-seq data in TCGA. Survival-related SF genes were identified by univariate Cox regression analysis. Spearman correlation analysis was performed to evaluate the correlation between the expression of survival-related SF genes and the PSI values of survival-related AS events. The SF-AS interaction network was generated by Cytoscape (version 3.7), with correlation coefficients greater than an absolute value of 0.8.

## 2.10 | Statistical analysis

All statistical analyses were performed using R software version 4.0.2. A $p$ value $< 0.05$ was considered statistically significant.

# 3 | RESULTS

## 3.1 | Integrated AS event profiles in PHC

Integrated AS event profiles were analysed for 130 patients with PHC obtained from the TCGA cohort. The detailed clinical characteristics of these patients with PHC are summarised in Table 1. Our results revealed that one gene might have different types of splicing patterns, which have great potential responsibility for transcriptome diversity. Additionally, ES splicing was the predominant type in PHC. To investigate the prognostic value of AS events in PHC patients, we conducted univariate Cox regression analysis to acquire OS-AS events. Consequently, 1684 AS events were identified as candidate OS-AS events with a $p$ value of $< 0.05$, and ES splicing remained the major AS pattern, accounting for more than one-third of the OS-AS events in PHC (Figure 1a,b). The top 20 most significant prognostic AS events for each pattern are displayed in Figure 2a–g. Obviously, many of the top 20 AS events in AA, AD, and RI acted as favourable prognostic elements (Z-score $< 0$). In addition, we noticed that one gene might have two or more OS-AS events that showed the same or opposite effect on survival. For example, AD, ES ,and RI events in the *IL32* gene were significantly associated with OS and had favourable or adverse effects on PHC survival.

## 3.2 | Identification of two clusters based on prognostic AS events

The OS-AS events were subjected to NMF clustering analysis. A desired rank $k$ was utilised to determine the numbers of clusters. The most common approach to determine the $k$ value is based on the cophenetic correlation coefficient. We use the minimum $k$ value at which the cophenolic correlation coefficient begins to drop. For the silhouette coefficient, many studies reported that the closer it is to one, the better the clustering result is. However, when the silhouette coefficient is maximum, the error is also maximum. After a comprehensive consideration, $k = 2$ was selected as the optimal cluster number (Figure S1a,b), that is, assigning the patients with PHC into two clusters (cluster 1 and 2). As shown in Figure 3a, the

**TABLE 1** Clinical characteristics of the melanoma patients used in the present study

| Clinical characteristics | TCGA cohort |
| --- | --- |
| No. of patients | 130 |
| Age (years) (mean, SD) | 64.16 (10.86) |
| Gender (%) | |
| Male | 69 (53.08%) |
| Female | 61 (46.92%) |
| History (%) | |
| Tobacco history | 59 (45.38%) |
| Alcohol history | 72 (55.38%) |
| Family history | 44 (33.85%) |
| History of chronic pancreatitis | 10 (7.69%) |
| History of diabetes | 29 (22.31%) |
| Grade (%) | |
| Grade 1 | 20 (15.38%) |
| Grade 2 | 75 (57.69%) |
| Grade 3 | 34 (26.15%) |
| Grade 4 | 0 (0) |
| Unknown | 1 (0.77%) |
| Residual (%) | |
| R0 | 74 (56.92%) |
| R1 | 43 (33.08%) |
| R2 | 4 (3.08%) |
| Unknown | 4 (3.08%) |
| Not available | 5 (3.85%) |
| Stage (%) | |
| I | 12 (9.23%) |
| II | 113 (86.92%) |
| III | 4 (3.08%) |
| IV | 1 (0.77%) |

consensus matrix heatmap for two clusters had sharp and clear edges, indicating excellent clustering stability and robustness. Furthermore, the survival analysis showed that the patients in cluster 1 had significantly shorter OS and PFS than patients in cluster 2 ($p < 0.001$) (Figure 3b,c).

## 3.3 | The relationship between AS clusters and tumour immunity

We investigated the infiltration differences of 10 immune cells by the MCP-counter method between cluster 1 and cluster 2. As shown in Figure 3d, cluster 1 patients had significantly lower proportions of B cells, CD8 T cells, cytotoxic lymphocyte (CTL), endothelial cells, fibroblast, fibroblast, myeloid

dendritic cells, NK cells, and T cells. These results suggested that PHC patients in cluster 1 display lower immune cell infiltration. In addition, we investigated the relationship between our clusters and the global transcriptomic immune classification (C1–C6) as described above. The results showed that cluster 1 tended to be immune C1 and C2 types, while cluster 2 tended to be immune C3 and C6 types (Figure 3e). In summary, the two innovative subtypes we identified were significantly associated with unique immune characteristics.

## 3.4 | Discovering AS signatures for PHC

LASSO Cox regression analysis was used to select the key OS-AS events as candidates from the seven types (Figure S2a). Based on the optimal value of $\lambda$, an AS-related prognostic signature was constructed (Figure S2b), including seven AS events (Table S1). The heatmap for these PSI values of seven AS events is shown in Figure 4a. According to the cut-off point value, 130 patients with PHC were divided into the high-risk group ($N = 65$) and the low-risk group ($N = 65$). Additionally, Figure 4b,c was generated to show the risk score and survival status of each PHC patient, indicating that the clinical outcome of patients in the high-risk group was worse than those in the low-risk group. The Kaplan–Meier survival analysis showed that the patients in the low-risk group exhibited significantly longer OS and PFS than those in the high-risk group (Figure 4d,e). The AUC-ROC of the prognostic signature calculated from TCGA was 0.842 at 1 year, 0.853 at 2 years, and 0.789 at 3 years, indicating that the AS-related prognostic signature exhibited good performance in monitoring survival (Figure 4f). The prediction performance of the model varies with the evaluation time, and it has the best prediction effect on a 2-year survival. This shows that the AS-related prognostic signature can be used as an effective tool to predict the survival of PHC patients in the clinic. Subsequently, we compared the AUC-ROC of the risk score with that of other clinical parameters. The results showed that the risk score was superior to other clinical parameters (Figure 5a). To further illustrate the advantages of the AS-related risk score, we established a prognostic signature based on seven genes corresponding to AS events involved in the final signature. As shown in Figure S4, the AUC-ROC of the prognostic signature was 0.740 at 1 year, 0.708 at 2 years, and 0.735 at 3 years. Compared with this, the AS-related signature has better performance in predicting OS for PHC.

Additionally, seven prognostic models for each AS type were also developed by LASSO Cox regression analysis, with 14 AS events in AAs, nine in ADs, seven in APs, seven in ATs, eight in ESs, five in MEs, and five in RIs. As shown in Figure S3a–g, the patients in the high-risk groups all had significantly shorter OS and PFS than those in the low-risk groups. It is worth mentioning that the AUCs of the seven signatures were all greater than 0.70 (Figure S5a–g). In summary, AS events have good potential in predicting the prognosis of patients with PHC. In the present study, we focussed on exploring all types of AS events in PHC. Therefore, the
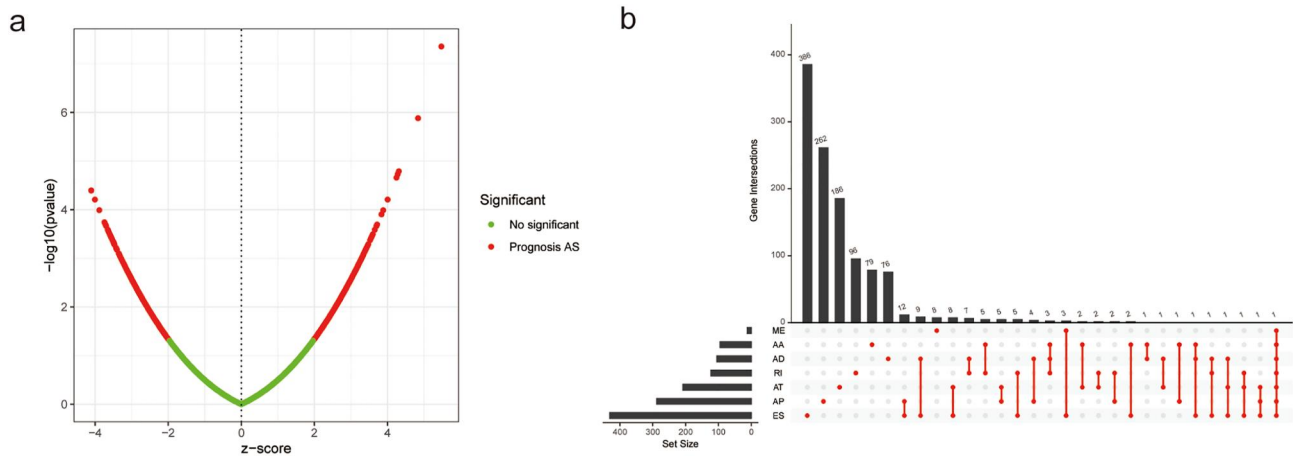
**FIGURE 1** Overall survival-related alternate splicing (OS-AS) events in PHC. (a) Volcano plot of OS-AS events (red dots) and survival-irrelated AS events (green dots). (b) UpSet plot of interactions between the seven types of OS-AS events in PHC. The left column shows the number of OS-AS events of each type. The right column shows the distribution of genes involved in OS-AS events. PHC, pancreatic head cancer.

signature established by all types of AS events was used in subsequent analyses.

We used univariate and multivariate Cox regression analyses to determine whether the risk score was an independent prognostic factor for PHC among clinicopathological factors. In univariate Cox regression analysis, age, grade, and risk score were significantly correlated with poor prognosis (Figure 5b). After correcting for other confounding factors, the grade and risk score still showed significant differences by multivariate Cox regression analysis, which indicated that the risk score was an independent prognostic factor for PHC (Figure 5c).

Additionally, we investigated the relationship between clinical parameters. The results showed that age, sex, and TNM stage did not significantly influence the risk score. Patients with G3 cancer showed a higher risk score than patients with G1 ($p = 0.001$) and G2 ($p = 0.023$) cancers (Figure 6a–g).

## 3.5 | Construction of a nomogram based on the AS prognostic signature

To easily predict the individualised survival probability of PHC patients, a graphical nomogram integrating the risk score of the signature and clinical parameters was established (Figure 7a). To assess the actual and predictive performance of the nomogram for 1, 2, and 3 years in PHC, calibration curves were plotted, which indicated a stable consistency between the predicted and actual survival (Figure 7b–d). In this sense, the nomogram with the AS risk score could be used as an effective tool to predict the survival of PHC patients in the clinic.

## 3.6 | Immune landscape of the final signature based on seven AS events

To understand the specific immune characteristics of the AS-related signature, we explored the differences in the

ESTIMATE score, stromal score, tumour purity, and immune score between the high- and low-risk groups. As shown in Figure 8a, the high-risk group showed lower ESTIMATE scores, immune scores, and stromal scores but higher tumour purity than the low-risk group. Subsequently, immune cell infiltration, immune-related pathways, and immune-related functions were evaluated by ssGSEA. We found lower immune cell infiltration in the high-risk group, including NK cells, CD8 T cells, CD4 T cells, regulatory T cells, B cells, mast cells, macrophages and so on. We found that the proportions of B cells, CD8 T cells, Th cells, macrophages, and DCs were significantly lower in the high-risk group. Additionally, the scores of APC costimulation, checkpoint, cytolytic activity, inflammation promotion, T-cell costimulation, T-cell coinhibition, and Type II IFN response were lower in the high-risk group (Figure 8a).

As mentioned above, there were differences in the checkpoint between the high- and low-risk groups. Thus, we assessed the association between the risk score and different immune checkpoint molecules. As shown in Figure 8b,c, the risk score was significantly correlated with PDCD1. Further analysis showed that the high-risk group had significantly lower expression of 20 immune genes, including PDCD1, than the low-risk group (Figure 8d).

## 3.7 | Regulatory network of survival-associated AS events

SFs can regulate AS events by recognising *cis*-regulatory elements within the pre-mRNA. Numerous studies have highlighted that the altered expression of SF genes can promote oncogenesis [22]. However, it is unknown whether these AS events may be regulated by prognostic SFs in PHC tissues. To provide further insights into the influences of SFs in PHC on RNA splicing, we constructed a regulatory network of survival-associated AS events. A correlation network was built using the
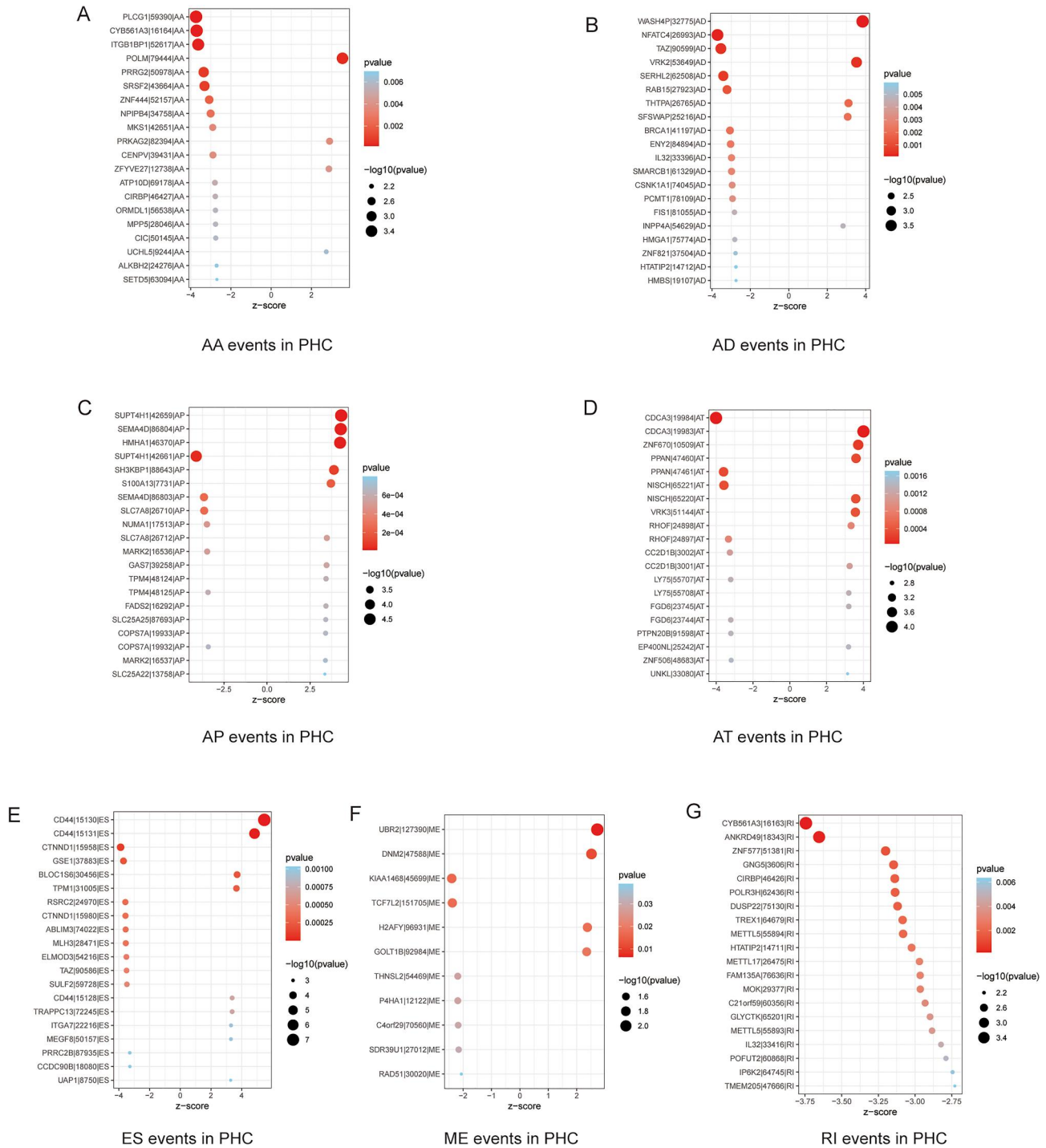
**FIGURE 2** Bubble plots for seven patterns of overall survival-related alternate splicing (OS-AS) events in PHC. (a) Bubble plots for the top 20 OS-alternate acceptor (AA) events. (b) Bubble plots for the top 20 OS-alternate donor (AD) events. (c) Bubble plots for the top 20 OS-alternate promoter (AP) events. (d) Bubble plots for the top 20 OS-alternate terminator (AT) events. (e) Bubble plots for the top 20 OS-exon skipping (ES) events. (f) Bubble plots for the top 20 OS-mutually exclusive exon (ME) events. (g) Bubble plots for the top 20 OS-retained intron (RI) events. $p$ values are indicated by the size of the bubble and the colour scale. There was a corresponding relationship between the $p$ value and Z-score. PHC, pancreatic head cancer.

Spearman correlation analysis, and significant correlations are presented in Figure 9. The results showed that the expression of 11 SF genes (green dots) was significantly correlated with 12 OS-AS events. Among these AS events, nine AS events were significantly linked with favourable survival (blue dots), while three AS events were significantly linked with adverse survival (red dots). These results indicated that these AS events were potentially regulated by a few key SFs related to prognosis in PHC tissues, which provided an in-depth understanding of the regulatory mechanisms in PHC.
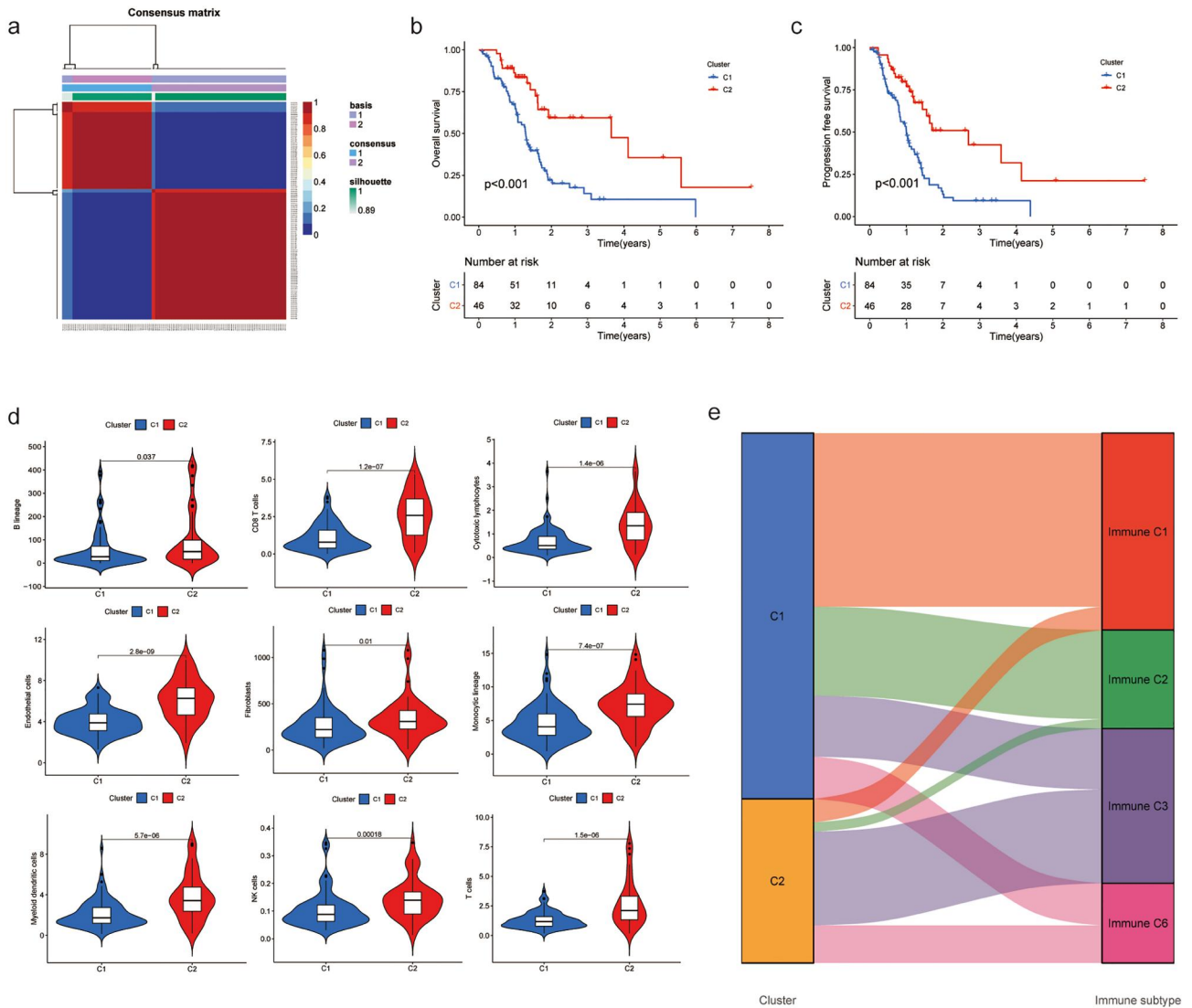
**FIGURE 3** Differences in tumour immunity between the two clusters based on overall survival-related alternate splicing (OS-AS) events. (a) Consensus matrix heatmap when $k = 2$. (b) Kaplan–Meier survival curve analysis for the overall survival (OS) of the two clusters. (c) Kaplan–Meier survival curve analysis for the progression-free survival (PFS) of the two clusters. (d) The landscape of immune cell infiltration in the two clusters. (e) A Sankey diagram for the correlation between two clusters and the global transcriptomic immune classification (C1–C6).

# 4 | DISCUSSION

PC is a common aggressive tumour with a high mortality rate. To date, the American Joint Committee on Cancer tumour-node-metastasis (AJCC-TNM) classification system is still the only indicator to assess the survival of PC in clinical practice [23]. However, the conventional classification cannot meet the need for precision medicine. With the development of high-throughput sequencing, an increasing number of prognostic factors have been proposed based on genomic analysis [24]. However, the relevant research in PHC has not been carried out until now. Studies have revealed that right- and left-sided colon cancer have different risk factors and molecular and biological characteristics. These results suggested that mechanisms in carcinogenesis might differ with tumour location [25, 26]. Increasing evidence indicates that these differences also

exist between pancreatic head and body/tail cancers, providing decision-making support for different tumour locations in PC [27]. In this sense, it is necessary to explore the PHC mechanism. Therefore, we focussed on the identification of a prognostic signature in PHC, with the purpose of developing a more accurate predictive tool for clinical practice.

Substantial evidence suggests that aberrant AS events are frequently observed in cancers and recognised as one of the most important prognostic signatures. These events play regulatory roles in the mechanism of cancers, such as promoting proliferation, metastasis, and drug resistance [28, 29]. Many studies have characterised survival-related AS events in PC [30, 31]. However, systematic survival analyses of AS events in PHC have been lacking thus far. In the present study, we analysed AS events in PHC and identified survival-relevant AS events as candidate factors to construct the
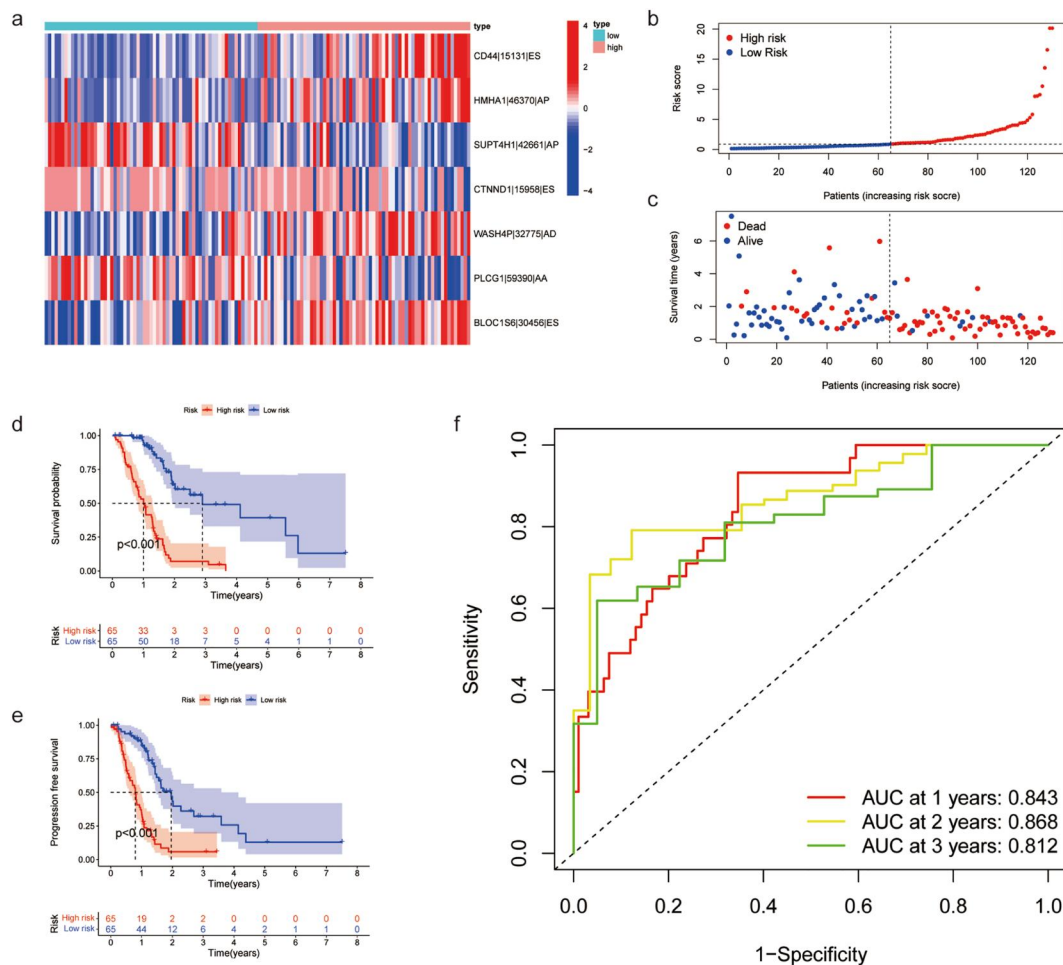
**FIGURE 4** Identification and assessment of an alternate splicing (AS)-related prognostic signature for PHC. (a) Heatmap of AS events included in the prognostic signature in the low- and high-risk groups. (b) The distribution and median value of the risk scores. Patients were divided into low- and high-risk groups based on the median value. (c) The scatter plot of survival overview. The red dots indicate death, and the green dots indicate survival. (d) Kaplan–Meier survival curve analysis for the overall survival (OS) of the prognostic signature for PHC. (e) Kaplan–Meier survival curve analysis for the progression-free survival (PFS) of the prognostic signature for PHC. (f) The receiver operating characteristic (ROC) curve for assessing the predictive ability of the risk score based on the prognostic signature in PHC. PHC, pancreatic head cancer.

prognostic signature. Among the seven types of AS events associated with OS, ES events were the most important splicing pattern. Additionally, it has been reported that ES events are also the predominant type in breast cancer and prostate cancer [32, 33]. These findings suggested that ES events might be primarily responsible for the complexity of the proteome and biological activity in cancer. CD44|15130 and CD44|15131 ranked top in the list of AS events and were significantly associated with OS of PHC. Interestingly, it was consistent with the finding in PC [30]. CD44, a PC stem cell marker, undergoes AS to generate CD44 standard and CD44 variants (CD44v) [34]. CD44v expression has been demonstrated to increase in PC, which was associated with PC metastasis and progression [34]. CD44v expression has been demonstrated to increase in PC, which was associated with PC metastasis and progression [34]. Furthermore, BRCA1|41197 was one of the top 20 OS-AS events of the AD pattern. BRCA1 variants were proven to be pathogenic in PC and were related to DNA damage repair [35]. In this

regard, these findings also verified the accuracy of the results in this study. However, the molecular mechanisms of OS-AS events in PHC remain largely unstudied.

In the present study, two clusters with different prognoses were identified according to the PSI values of OS-AS events. Cluster 2 had a higher immune cell infiltration than cluster 1. In addition, there was a relationship between the clusters and the immune classification identified by Thorsson V et al. (C1–C6) [19]. Cluster 1 mainly corresponded to the immune C1 type (wound healing), while cluster 2 mainly corresponded to the immune C3 type (inflammatory). Among the six immune types, C3 had the best prognosis, while C1 had less favourable outcomes. These findings were consistent with our results. Therefore, the AS-related classifier with prognostic value could determine the specific subtypes associated with tumour immunity in PHC.

However, the AS-related classifier based on the NMF clustering method could not be applied to individual PHC patients. Thus, we performed a systematic analysis to construct
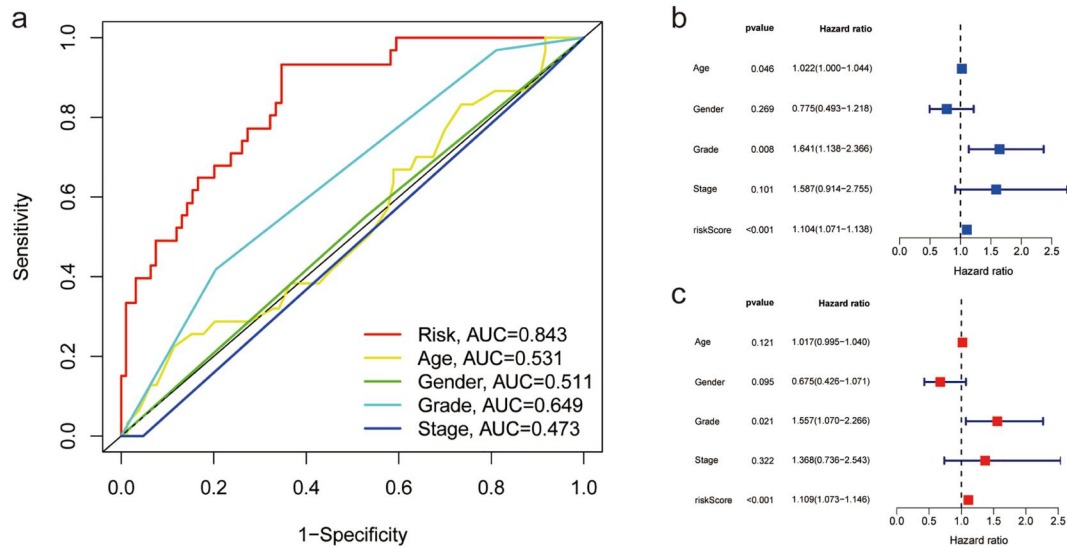
**FIGURE 5** Cox regression analyses for evaluating the independent prognostic value of the risk score. (a) The receiver operating characteristic (ROC) curves for risk score, age, sex, grade, and TNM stage. (b) Univariate Cox regression analysis of the association between survival and clinicopathological features as well as risk score. (c) Multivariate Cox regression analysis of the association between survival and clinical features as well as risk score. Horizontal bars represent 95% confidence intervals.
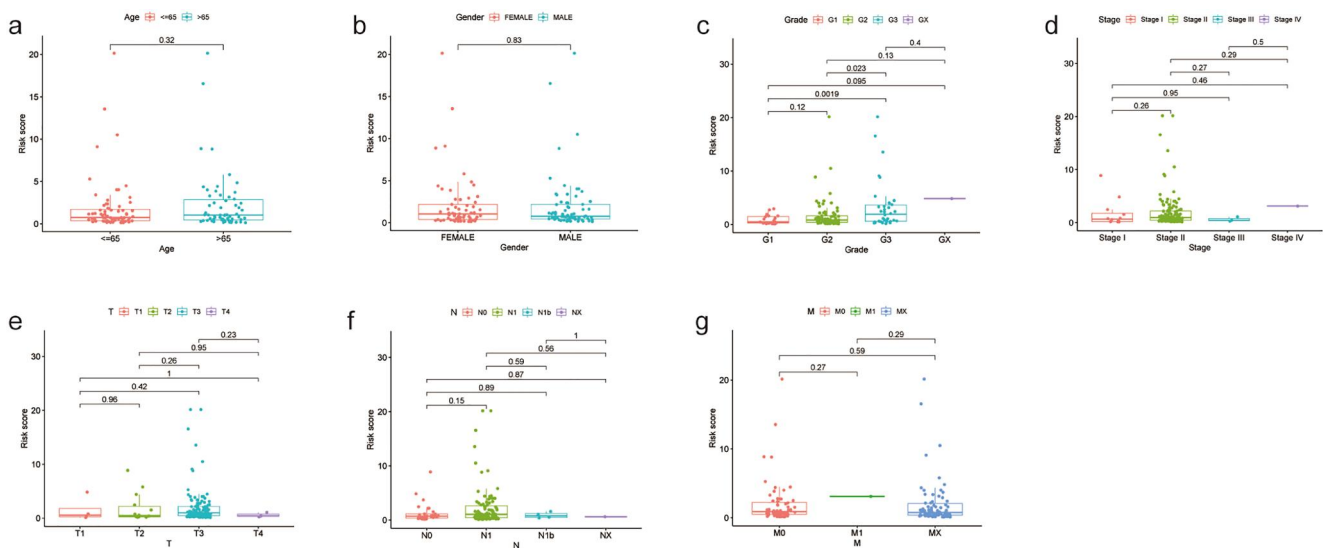


**FIGURE 6** The relationship between clinical features and risk score. (a) The relationship between age and risk score. (b) The relationship between sex and risk score. (c) The relationship between grade and risk score. (d) The relationship between stage and risk score. (e) The relationship between T stage and risk score. (f) The relationship between N stage and risk score. (g) The relationship between M stage and risk score.

a signature based on OS-AS events to assess the prognosis in individuals. The AUCs of the AS signature were 0.843 at 1 year, 0.868 at 2 years, and 0.812 at 3 years. The results suggested that the newly established signature performed well in PHC. More importantly, the risk score was verified as an independent prognostic factor for patients with PHC. In addition, we established a nomogram combining age, sex, TNM stage, and risk score, which showed a good predictive performance. Nomograms, transforming statistical predictive models into a single numerical estimate of survival in each cancer patient, have become powerful and easily applicable tools in clinical

practice [36]. Additionally, nomograms have been confirmed to be better than risk stratification, artificial neural networks (ANNs), and other predictive models [37]. Hence, the newly established nomogram based on the AS risk score has great potential in clinical applications.

Increasing evidence indicates that AS events can regulate immune activity by producing different transcriptional isoforms to supplement the function of immunity-related genes [38]. Aberrant AS events are commonly observed in cancers and have been demonstrated to play a critical role in the antitumour immune response [39]. In this sense,
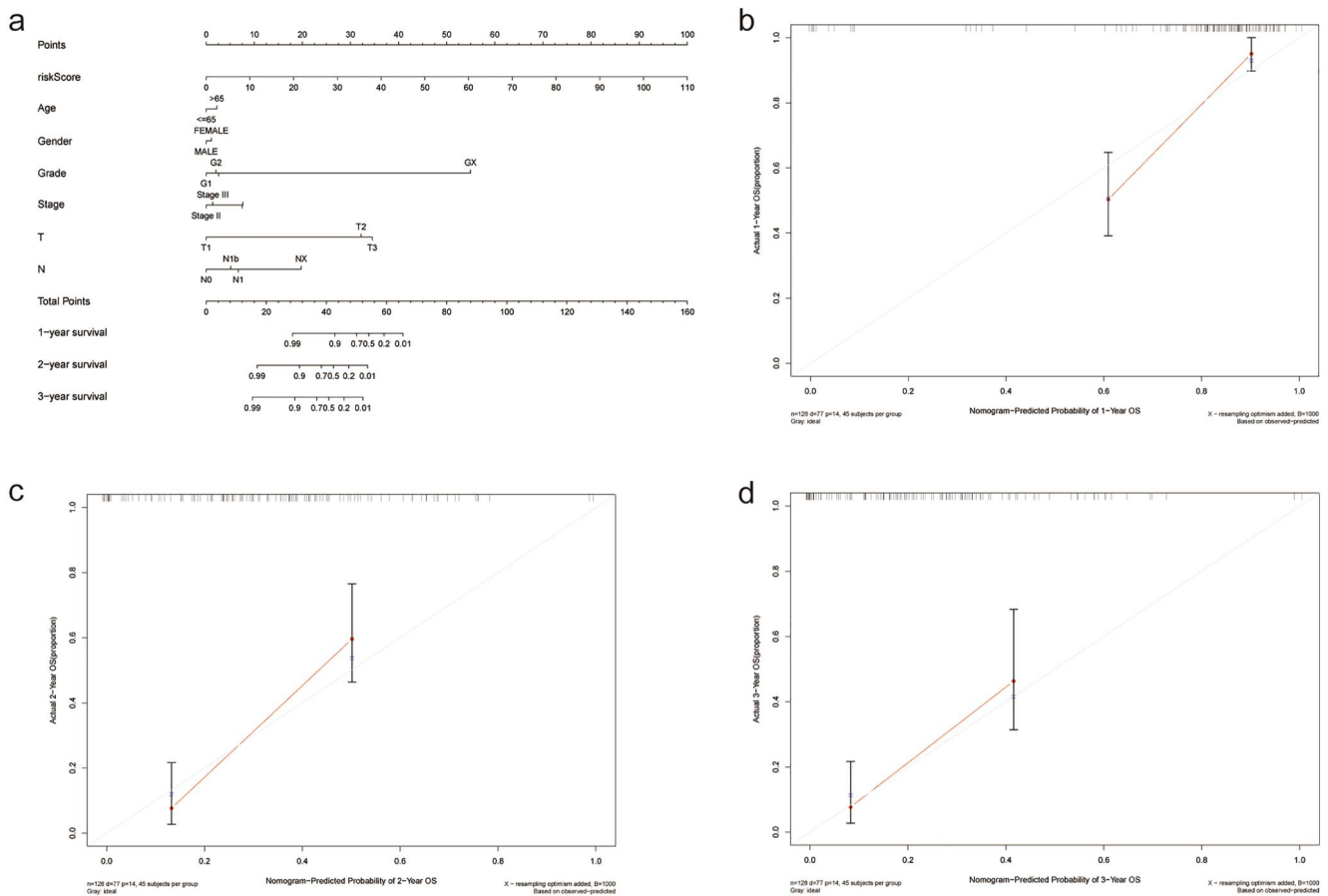
**FIGURE 7** Establishment and assessment of a nomogram integrating the risk score and clinicopathological features. (a) Nomogram for predicting the 1-, 2- and 3-year survival in patients with pancreatic head cancer (PHC). The scores for all parameters were added and translated into 1-, 2- and 3-year survival rates. (b) Calibration curve of the nomogram for 1-year survival. (c) Calibration curve of the nomogram for 2-year survival. (d) Calibration curve of the nomogram for 3-year survival.

dysregulated AS events in cancers lay the foundation for immune-therapy target expansion. As mentioned above, there were significant differences in the immune cell infiltration of cluster 1 and cluster 2. Therefore, we explored the association between the risk score and tumour immunity in PHC. In this study, the high-risk patients had lower proportions of B cells, CD8+ T cells, and Tregs. Many studies have shown that the proportion of Treg cells is positively related to the poor prognosis of PC patients, which is inconsistent with our results [40]. However, recent studies reported that the depletion of Treg cells led to the acceleration of tumour progression in PC, which might explain the lower proportion of Tregs in the high-risk group [41]. Treg cells suppress CD8+ T cells in numerous ways. Nevertheless, the increase in CD8+ T cells caused by Treg depletion was offset by a compensatory increase in other cells [41]. Additionally, it was important to mention that the scores of APC costimulation and T-cell costimulation were lower in the high-risk group, which contributed to immune evasion. Immune evasion has been considered one of the hallmarks of cancer. To avoid immune recognition and destruction, the abnormal regulation of antigen-presenting molecules causes damage to T-cell responses [42]. It has been reported that downregulation or loss of antigen-presenting molecules was observed frequently in PC [43]. Thus, our results have important implications for further understanding the mechanism of AS events in promoting PHC tumourigenesis.

Immune checkpoint inhibitors have expressed a remarkable potential in the treatment of cancer. However, they are rarely effective for PC, and only patients with different mismatch repair or microsatellite instability were recommended to treat with anti-PD-L1 [44]. Several studies found a correlation between the expression of immune checkpoint genes and response to immunotherapy or cancer prognosis [45]. Thus, we further explored the relationship between immune checkpoint genes and the risk score. The results showed that the high-risk group had significantly lower immune checkpoint gene expression, including PDCD1. In summary, immune analysis found that PHC patients in the high-risk group exhibited lower immune scores, lower CD8 T and Th-cell infiltration, and lower immune checkpoint gene expression. It has been reported that anticancer immunity is generally characterised into three main phenotypes: the
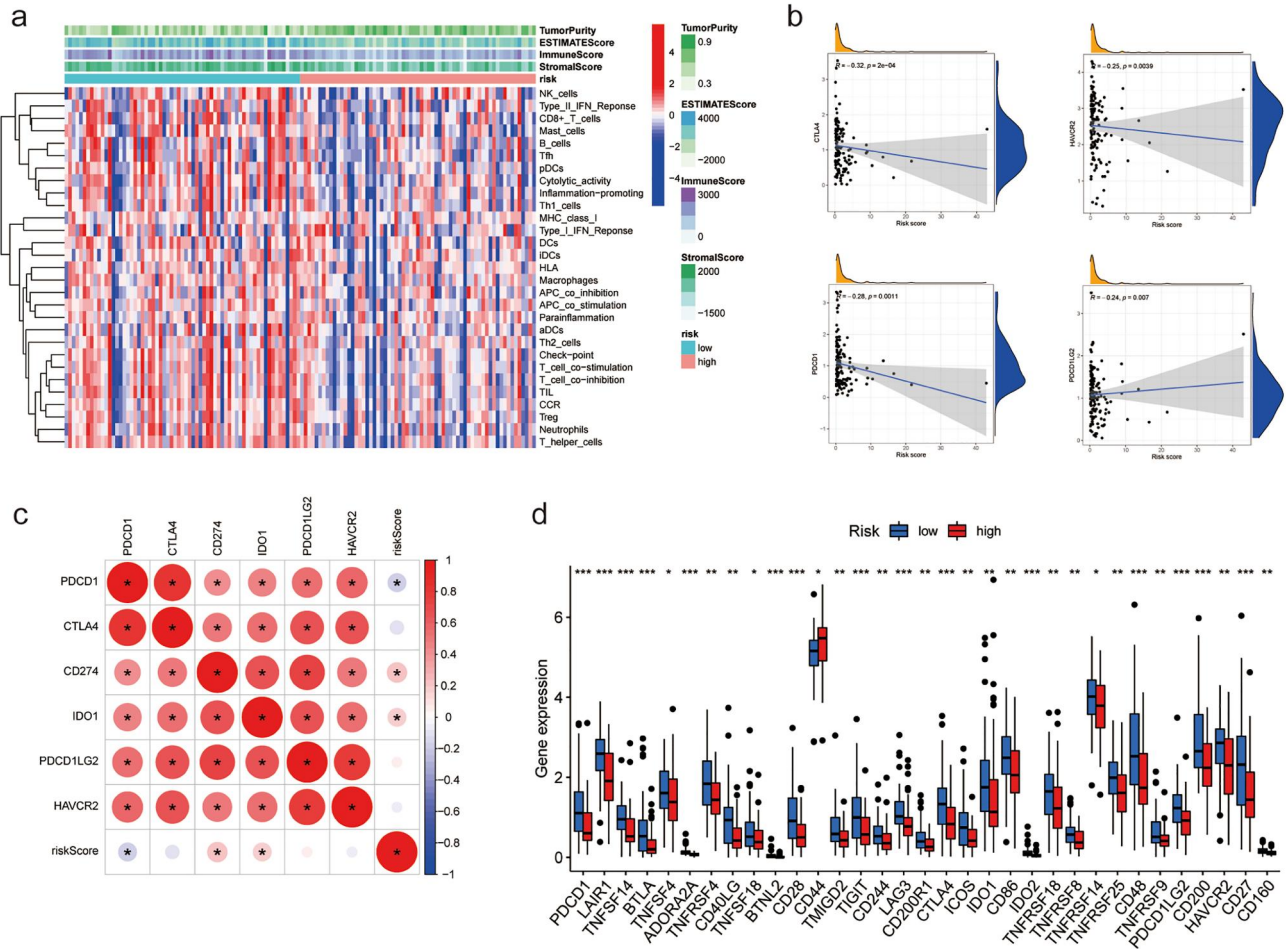
**FIGURE 8** Immune landscape of the AS-related signature in pancreatic head cancer (PHC). (a) Top: difference in ESTIMATE score, immune score, stromal score, and tumour purity between the high- and low-risk groups. Bottom: The heatmap displays the differences in immune cell infiltration and immune function between the high- and low-risk groups. (b) Correlation between the risk score and CTLA-4, HAVCR2, PDCD1, and PDCD1LG2. (c) Correlation matrix of the risk score and main immune checkpoint genes. (d) Comparison of the expression of 20 immune checkpoint genes between the low- and high-risk groups.

inflamed phenotype, the immune-excluded phenotype and the immune-desert phenotype, which are associated with individual responses to anti-PD-L1/PD-1 therapy [46]. The immune-desert phenotype is characterised by a lack of T cells in either the tumour cells or the stroma, which rarely respond to anti-PD-L1/PD-1 therapy [47]. Unsurprisingly, the high-risk group was more likely to be this immune-desert phenotype. Thus, it was reasonable to speculate that the patients in the high-risk group might have a weaker response to immunotherapy. In this sense, the established risk score could serve as a predictor for the prognosis and response to immunotherapy, which provides support for clinical decision-making.

Although our results showed promise and potential, there were still some limitations and shortcomings in the present study. First, due to the lack of datasets containing all information needed for further analysis, we analysed only the data from TCGA. Furthermore, we utilised published retrospective datasets for the analysis, and these results were not validated in prospective studies. In the future, we will collect clinical samples for external validation in an attempt to confirm the clinical application value of the signature.

## 5 | CONCLUSION

In the present study, we integrated AS event profiles in PHC and identified a novel risk score associated with tumour immunity that exhibited good performance in predicting the prognosis of PHC. The SF network provided reliable information to better understand the mechanism of AS events in oncogenesis in PHC.
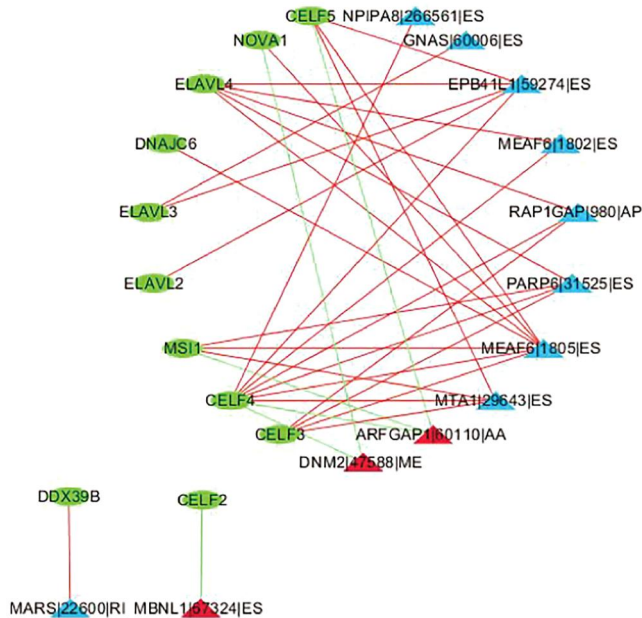
### AUTHOR CONTRIBUTION

**FIGURE 9** Construction of the regulatory splicing factor (SF)-alternative splicing (AS) network in PHC. AS events with different survival statuses are marked in blue (favourable survival) or red (adverse survival). SFs (green dots) positively (red lines) or negatively (green lines) regulate AS events.

## ACKNOWLEDGEMENT
None.

## CONFLICT OF INTEREST
The authors have no conflicts of interest to declare.

## DATA AVAILABILITY STATEMENT
The datasets presented in this study can be found in online repositories (The Cancer Genome Atlas [TCGA] and TCGASpliceSeq).

## ORCID
*Lingshan Zhou* https://orcid.org/0000-0002-0095-3376
*Chengdong Qiao* https://orcid.org/0000-0003-1379-261X

## REFERENCES
1. Rahib, L., et al.: Projecting cancer incidence and deaths to 2030: the unexpected burden of thyroid. Cancer Res. 74(11), 2913–21 (2014). https://doi.org/10.1158/0008-5472.can-14-0155
2. Sung, H., et al.: Global cancer statistics 2020: GLOBOCAN estimates of incidence and mortality. CA Cancer J. Clin. 71(3), 209–249 (2021). https://doi.org/10.3322/caac.21660
3. Mizrahi, J.D., et al.: Pancreatic cancer. Lancet 395(10242), 2008–2020 (2020). https://doi.org/10.1016/s0140-6736(20)30974-0
4. Ling, Q., et al.: The diversity between pancreatic head and body/tail cancers: clinical parameters and. Hepatobiliary Pancreat. Dis. Int. 12(5), 480–487 (2013). https://doi.org/10.1016/s1499-3872(13)60076-4
5. Winer, L.K., et al.: The impact of tumor location on resection and survival for pancreatic ductal adenocarcinoma. J. Surg. Res. 239, 60–66 (2019). https://doi.org/10.1016/j.jss.2019.01.061
6. Mackay, T.M., et al.: Association between primary origin (head, body and tail) of metastasised pancreatic ductal adenocarcinoma and oncologic outcome: a population-based analysis. Eur. J. Cancer 106, 99–105 (2019). https://doi.org/10.1016/j.ejca.2018.10.008
7. van Erning, F.N., et al.: Association of the location of pancreatic ductal adenocarcinoma (head, body, tail). Acta Oncol. 57(12), 1655–1662 (2018). https://doi.org/10.1080/0284186X.2018.1518593
8. Jones, S., et al.: Core signaling pathways in human pancreatic cancers revealed by global genomic. Science 321(5897), 1801–1806 (2008). https://doi.org/10.1126/science.1164368
9. Biankin, A.V., et al.: Pancreatic cancer genomes reveal aberrations in axon guidance pathway genes. Nature 491(7424), 399–405 (2012). https://doi.org/10.1038/nature11547
10. Dreyer, S.B., et al.: Defining the molecular pathology of pancreatic body and tail adenocarcinoma. Br. J. Surg. 105(2), e183–e191 (2018). https://doi.org/10.1002/bjs.10772
11. Kornblihtt, A.R., et al.: Alternative splicing: a pivotal step between eukaryotic transcription and. Nat. Rev. Mol. Cell Biol. 14(3), 153–65 (2013). https://doi.org/10.1038/nrm3525
12. Keren, H., Lev-Maor, G., Ast, G.: Alternative splicing and evolution: diversification, exon definition and function. Nat. Rev. Genet. 11(5), 345–355 (2010). https://doi.org/10.1038/nrg2776
13. Cherry, S., Lynch, K.W.: Alternative splicing and cancer: insights, opportunities, and challenges from an. Genes Dev. 34(15–16), 1005–1016 (2020). https://doi.org/10.1101/gad.338962.120
14. Calabretta, S., et al.: Modulation of PKM alternative splicing by PTBP1 promotes gemcitabine resistance in. Oncogene 35(16), 2031–2039 (2016). https://doi.org/10.1038/onc.2015.270
15. Li, M., et al.: miR-193a-5p promotes pancreatic cancer cell metastasis through SRSF6-mediated. Am. J. Cancer Res. 10(1), 38–59 (2020)
16. Kędzierska, H., Piekiełko-Witkowska, A.: Splicing factors of SR and hnRNP families as regulators of apoptosis in cancer. Cancer Lett. 396, 53–65 (2017). https://doi.org/10.1016/j.canlet.2017.03.013
17. Nie, H., et al.: The short isoform of PRLR suppresses the pentose phosphate pathway and nucleotide. Theranostics 11(8), 3898–3915 (2021). https://doi.org/10.7150/thno.51712
18. Ryan, M.C., et al.: SpliceSeq: a resource for analysis and visualization of RNA-Seq data on alternative. Bioinformatics 28(18), 2385–2387 (2012). https://doi.org/10.1093/bioinformatics/bts452
19. Thorsson, V., et al.: The immune landscape of cancer. Immunity 48(4), 812–830.e14 (2018). https://doi.org/10.1016/j.immuni.2018.03.023
20. Mak, M.P., et al.: A patient-derived, pan-cancer EMT signature identifies global molecular alterations and immune target enrichment following epithelial-to-mesenchymal transition. Clin. Cancer Res. 22(3), 609–620 (2016). https://doi.org/10.1158/1078-0432.ccr-15-0876
21. Seiler, M., et al.: Somatic mutational landscape of splicing factor genes and their functional. Cell Rep. 23(1), 282–296.e4 (2018)
22. Lee, S.C., Abdel-Wahab, O.: Therapeutic targeting of splicing in cancer. Nat. Med. 22(9), 976–986 (2016). https://doi.org/10.1038/nm.4165
23. van Roessel, S., et al.: International validation of the Eighth Edition of the American Joint Committee on. JAMA Surg. 153(12), e183617 (2018). https://doi.org/10.1001/jamasurg.2018.3617
24. Le, N., et al.: Prognostic and predictive markers in pancreatic adenocarcinoma. Dig. Liver Dis. 48(3), 223–230 (2016). https://doi.org/10.1016/j.dld.2015.11.001
25. Snaebjornsson, P., et al.: Colon cancer in Iceland–a nationwide comparative study on various pathology parameters with respect to right and left tumor location and patients age. Int. J. Cancer 127(11), 2645–2653 (2010). https://doi.org/10.1002/ijc.25258
26. Slattery, M.L., et al.: MicroRNAs and colon and rectal cancer: differential expression by tumor location and subtype. Genes Chromosomes Cancer 50(3), 196–206 (2011). https://doi.org/10.1002/gcc.20844
27. Birnbaum, D.J., et al.: Head and body/tail pancreatic carcinomas are not the same tumors. Cancers 11(4), 497 (2019). https://doi.org/10.3390/cancers11040497
28. Climente-González, H., et al.: The functional impact of alternative splicing in cancer. Cell Rep. 20(9), 2215–2226 (2017). https://doi.org/10.1016/j.celrep.2017.08.012
29. Ule, J., Blencowe, B.J.: Alternative splicing regulatory networks: functions, mechanisms, and evolution. Mol. Cell 76(2), 329–345 (2019). https://doi.org/10.1016/j.molcel.2019.09.017

30. Lu, J., et al.: Systematic analysis of alternative splicing landscape in pancreatic adenocarcinoma reveals regulatory network associated with tumorigenesis and immune response. Med. Sci. Mon. Int. Med. J. Exp. Clin. Res. 26, e925733 (2020). https://doi.org/10.12659/msm.925733

31. Yao, J., et al.: Signature of gene aberrant alternative splicing events in pancreatic adenocarcinoma prognosis. J. Cancer 12(11), 3164–3179 (2021). https://doi.org/10.7150/jca.48661

32. Eswaran, J., et al.: RNA sequencing of cancer reveals novel splicing alterations. Sci. Rep. 3(1), 1689 (2013). https://doi.org/10.1038/srep01689

33. Huang, Z.G., et al.: Prognostic value and potential function of splicing events in prostate. Int. J. Oncol. 53(6), 2473–2487 (2018). https://doi.org/10.3892/ijo.2018.4563

34. Li, Z., et al.: CD44v/CD44s expression patterns are associated with the survival of pancreatic. Diagn. Pathol. 9(1), 79 (2014). https://doi.org/10.1186/1746-1596-9-79

35. Zhan, W., et al.: Germline variants and risk for pancreatic cancer: a systematic review and emerging. Pancreas 47(8), 924–936 (2018). https://doi.org/10.1097/mpa.0000000000001136

36. Iasonos, A., et al.: How to build and interpret a nomogram for cancer prognosis. J. Clin. Oncol. 26(8), 1364–1370 (2008). https://doi.org/10.1200/jco.2007.12.9791

37. Gondo, O.T., et al.: Nomogram as predictive model in clinical practice. Gan To Kagaku Ryoho 36(6), 901–906 (2009)

38. Su, Z., Huang, D.: Alternative splicing of pre-mRNA in the control of immune activity. Genes 12(4), 574 (2021). https://doi.org/10.3390/genes12040574

39. Bonnal, S.C., Lopez-Oreja, I., Valcarcel, J.: Roles and mechanisms of alternative splicing in cancer – implications for care. Nat. Rev. Clin. Oncol. 17(8), 457–474 (2020). https://doi.org/10.1038/s41571-020-0350-x

40. Tang, Y., et al.: An increased abundance of tumor-infiltrating regulatory T cells is correlated with. PLoS One 9(3), e91551 (2014). https://doi.org/10.1371/journal.pone.0091551

41. Zhang, Y., et al.: Regulatory T-cell depletion alters the tumor microenvironment and accelerates. Cancer Discov. 10(3), 422–439 (2020). https://doi.org/10.1158/2159-8290.cd-19-0958

42. Reeves, E., James, E.: Antigen processing and immune regulation in the response to tumours. Immunology 150(1), 16–24 (2017). https://doi.org/10.1111/imm.12675

43. Pandha, H., et al.: Loss of expression of antigen-presenting molecules in human pancreatic cancer and. Clin. Exp. Immunol. 148(1), 127–135 (2007). https://doi.org/10.1111/j.1365-2249.2006.03289.x

44. Li, J., et al.: Tumor cell-intrinsic factors underlie heterogeneity of immune cell infiltration and response to immunotherapy. Immunity 49(1), 178–193.e7 (2018). https://doi.org/10.1016/j.immuni.2018.06.006

45. Henriksen, A., et al.: Checkpoint inhibitors in pancreatic cancer. Cancer Treat Rev. 78, 17–30 (2019). https://doi.org/10.1016/j.ctrv.2019.06.005

46. Chen, D.S., Mellman, I.: Elements of cancer immunity and the cancer-immune set point. Nature 541(7637), 321–330 (2017). https://doi.org/10.1038/nature21349

47. Herbst, R.S., et al.: Predictive correlates of response to the anti-PD-L1 antibody MPDL3280A in cancer patients. Nature 515(7528), 563–7 (2014). https://doi.org/10.1038/nature14011

## SUPPORTING INFORMATION

Additional supporting information can be found online in the Supporting Information section at the end of this article.

**How to cite this article:** Zhou, L., et al.: Comprehensive analysis of alternative splicing signatures in pancreatic head cancer. IET Syst. Biol. 17(1), 14–26 (2023). https://doi.org/10.1049/syb2.12056